Colloids and Surfaces B: Biointerfaces 159 (2017) 303–311

Contents lists available at ScienceDirect

Colloids and Surfaces B: Biointerfaces

journal homepage: www.elsevier.com/locate/colsurfb

Full Length Article

Bioaccumulation and toxicity of CdSe/ZnS quantum dots in *Phanerochaete chrysosporium*

Liang Hu[a,b], Guangming Zeng[a,b,*], Guiqiu Chen[a,b,*], Zhenzhen Huang[a,b], Jia Wan[a,b], Anwei Chen[c], Zhigang Yu[a,b], Jiangli Yang[a,b], Kai He[a,b], Lei Qin[a,b]

[a] College of Environmental Science and Engineering, Hunan University, Changsha, Hunan 410082, PR China
[b] Key Laboratory of Environmental Biology and Pollution Control (Hunan University), Ministry of Education, Changsha, Hunan 410082, PR China
[c] College of Resources and Environment, Hunan Agricultural University, Changsha, Hunan 410128, PR China

ARTICLE INFO

Article history:
Received 26 May 2017
Received in revised form 28 July 2017
Accepted 2 August 2017
Available online 5 August 2017

Keywords:
CdSe/ZnS quantum dots
Toxicity
Reactive oxygen species
Confocal laser scanning microscopy
Phanerochaete chrysosporium

ABSTRACT

The growing potential of quantum dots (QDs) in biomedical applications has raised considerable concerns regarding their toxicological impact. Consequently, there has been a need to understand the underlying toxicity mechanism of QDs. In this work, we comprehensively investigated the bioaccumulation and toxicity of three CdSe/ZnS QDs (COOH CdSe/ZnS 525, NH_2 CdSe/ZnS 525, and NH_2 CdSe/ZnS 625) in *Phanerochaete chrysosporium* (*P. chrysosporium*) using confocal laser scanning microscopy, reactive oxygen species (ROS) measurements, and cell viability assays. Confocal laser scanning microscopy analytical results indicated that all the CdSe/ZnS QDs, with the concentration ranging from 10 to 80 nM, could accumulate largely in the hyphae and induce the generation of ROS, showing a direct toxicity to *P. chrysosporium*. And the bioaccumulation and toxicity of CdSe/ZnS QDs presented dose-dependent and time-dependent effects on *P. chrysosporium*. Furthermore, the CdSe/ZnS QDs-induced cytotoxicity was also related to their physicochemical properties, including particle size and surface charges: NH_2 CdSe/ZnS 525 with small size was more cytotoxic as compared to NH_2 CdSe/ZnS 625 with large size, and the smaller negative charged NH_2 CdSe/ZnS 525 resulted in greater cytotoxicity than the larger negative charged COOH CdSe/ZnS 525. The obtained results provide valuable information for exploring and understanding of toxicity mechanism of QDs in living cells.

1. Introduction

With the rapid development of nanotechnology over the past decades, nanomaterials have been extensively used in the fields of energy, environment, electronics, and biomedicine [1–7]. Quantum dots (QDs), as a functionalized nanomaterials, have been deemed to a new-type fluorescent probe and widely applied to biosensing, bioimaging, drug delivery, and cancer diagnostics, due to their unique advantages of narrow emission, broad excitation, high quantum yield, and excellent photostability [1,2,8,9]. A semiconductor core (e.g., CdS, CdSe, and CdTe) is the main component of a typical QD, and it can be encapsulated in a shell (e.g., ZnS) to enhance both electronic and optical properties and reduce core metal leaching [10,11]. Some QDs possess organic coatings which can increase their biocompatibility in water and help direct them to biological systems. However, the biosafety of QDs has been an intractable problem when QDs move into the clinical application because of their potential cytotoxicity.

In recent years, it has been confirmed that the cytotoxicity of QDs would lead to cell growth inhibition, mitochondrial dysfunction, DNA damage, and apoptosis [12–14]. The physicochemical properties of QDs, including core composition, size, surface charges, and functionalization would influence their toxicity to a great extent [15–17]. For instance, Soenen et al. [18] found that the cytotoxicity of QDs was correlated with the particle size, and the smaller QDs resulted in greater toxicity. Su et al. [19] reported that CdTe/CdS/ZnS QDs showed no cytotoxicity to cells while CdTe and CdTe/CdS QDs increased the intracellular reactive oxygen species (ROS) level and caused a decrease in cell viability, indicating that the ZnS shell could reduce the toxicity of CdTe QDs. Furthermore, Nagy et al. [13] carried out a comprehensive analysis to investigate the toxicity effects of sizes, surface charges, and functional groups of CdSe QDs on primary human lung cells. Results turned out that surface charges were considered to be the key factor that

* Corresponding authors at: College of Environmental Science and Engineering, Hunan University, Changsha, Hunan 410082, PR China.
E-mail addresses: zgming@hnu.edu.cn (G. Zeng), gqchen@hnu.edu.cn (G. Chen).

http://dx.doi.org/10.1016/j.colsurfb.2017.08.006
0927-7765/

responsible for the toxicity of QDs while sizes and functional groups played a lesser role.

To further explore and elucidate the cytotoxicity of QDs, many research groups have concentrated their attention on the mechanism study [20–23]. It has been widely believed that the release of toxic Cd^{2+} and the generation of ROS are the main reasons for QDs cytotoxicity [12,24]. Since Cd^{2+} can be released during the oxidation of QDs and bind to the sulfhydryl groups in many intracellular proteins, it may result in the functionality reduction of various subcellular organelles [25–27]. QDs-induced ROS has been verified to cause metabolic functions loss, DNA nicking and break, and apoptosis [12,28,29]. However, it is difficult to thoroughly understand the potential toxicity mechanism of QDs since QDs-caused cytotoxicity is extremely complicated due to the nanosize effects and heavy metal components. Once exposed to the biological system, QDs are almost impossible to maintain their original forms, and the bioaccumulation process of QDs in cells may be a significant reason for the complexity of mechanism.

Phanerochaete chrysosporium (*P. chrysosporium*), a white-rot fungus, has been widely used for the treatment of toxic organic pollutants and heavy metals contained wastewater because of its excellent degradation and removal ability for xenobiotics and heavy metals, respectively [30–33]. As *P. chrysosporium* was sensitive to pollutants and it could respond quickly to the changes of external environments [31], the *P. chrysosporium* was employed as the target microorganism to explore the cytotoxicity of QDs. Moreover, the physiological responses of *P. chrysosporium* under QDs exposure are still limited. Particularly, the effects of QDs exposure on the resistance and adaptability of *P. chrysosporium* have not been reported in the literature yet.

In view of this, three different types of CdSe/ZnS QDs in this study were used to investigate their bioaccumulation and toxicity to *P. chrysosporium*. These extremely small and highly photoluminescent nanoparticles were characterized by photoluminescence (PL), UV–vis absorption, dynamic light scatterer (DLS), and transmission electronic microscopy (TEM), respectively. Scanning electron microscope (SEM) was used to observe the morphological changes of *P. chrysosporium*. Confocal laser scanning microscopy was applied to evaluate the bioaccumulation of CdSe/ZnS QDs in *P. chrysosporium* by generating ROS. In addition, the effects of incubation concentrations and incubation time on the bioaccumulation and toxicity of CdSe/ZnS QDs have also been evaluated in detail.

2. Materials and methods

2.1. Reagents and instruments

QDs used in this work were purchased from Wuhan Jiayuan Quantum Dots Company (Wuhan, China). The nanoparticles were preserved as 8 μM QD in 200 μL borate buffer solutions. Three QDs (COOH CdSe/ZnS 525, NH_2 CdSe/ZnS 525, and NH_2 CdSe/ZnS 625) were composed of cadmium selenide (CdSe) core and zinc sulfide (ZnS) shell and encapsulated within the uniform amphipathic polymer of polyethylene glycol (PEG) coating. The differences among the three types of QDs are the surface functional groups (i.e. —NH_2 and —COOH) and particle sizes. In this work, all reagents must be of analytical reagent grade and were purchased from Sigma (St. Louis, MO, USA). Ultrapure water produced by a Milli-Q system (18.25 MΩ cm^{-1}, Millipore, France) was used throughout the process.

CdSe/ZnS QDs were characterized by PL, UV–vis absorption, DLS, and TEM, respectively. PL measurements were performed using a fluorescence spectrometer (FluoroMax-4, Horiba Scientific, Tokyo, Japan). The PL quantum yield (QY) of samples was estimated using Rhodamine 6G (QY = 95%) in ethanol solution as a reference standard, which was freshly prepared to decrease the measurement error [34]. UV–vis absorption spectra were recorded with a Perkin Elmer Lambda 750 Near-infrared UV–vis spectrophotometer (Model UV-2550, Shimadzu, Japan). DLS analysis (hydrodynamic diameter and zeta (ζ) potential) was carried out using a DynaPro Dynamic Light Scatterer (Malvern Instruments). The TEM overview images were recorded with a Philips CM 200 electron microscope (JEOL JEM-3010, Japan) operated at 200 kV. UV-vis, PL, and DLS were performed with the concentration of CdSe/ZnS QDs (20 nM) in borate buffer solutions, and TEM was performed with the concentration of CdSe/ZnS QDs (80 nM) in borate buffer solutions.

2.2. P. chrysosporium culture

P. chrysosporium BKMF-1767 used in this work was obtained from the China Center for Type Culture Collection (Wuhan, China). The fungal spores were prepared by subculturing on potato dextrose agar slants. Fungal spore suspensions were obtained by dissolving spores into sterile ultrapure water, and the spore concentration was adjusted to 2.0×10^6 CFU mL^{-1} using a turbidimeter (WGZ-200, Shanghai, China). 3 mL of aqueous suspensions of fungal spores was inoculated into 200 mL Kirk's liquid culture medium in a 500 mL Erlenmeyer flask at 37 °C for 3 days' cultivation [35].

2.3. Incubation concentrations and time

0.2 g *P. chrysosporium* pellets were seeded into 10 mL centrifuge tubes and fresh borate buffer solutions containing different concentrations of CdSe/ZnS QDs (0, 10, 20, 50, and 80 nM) were added. Then these centrifuge tubes were placed in an orbital shaker (120 rpm) at 37 °C. After incubation for different durations (0, 3, 6, 9, 15, and 24 h), *P. chrysosporium* pellets were collected and washed three times with ultrapure water for ROS and cell viability assays.

2.4. Morphology observation

After 24 h of incubation, *P. chrysosporium* pellets were harvested from aqueous medium and washed three times with ultrapure water. Afterwards, the pellets were stored in a refrigerator at −20 °C overnight, and then dried in a vacuum freezing drying oven at −50 °C for 48 h. The photomicrographs of *P. chrysosporium* pellets were taken by using SEM (HELIOS NANOLAB 600i, America) to observe the morphological changes. The elemental compositions of *P. chrysosporium* pellets were analyzed by using energy disperse spectroscopy (HELIOS NANOLAB 600i, America) after gold plating at an accelerating voltage of 20 kV.

2.5. Confocal laser scanning microscopy

0.2 g *P. chrysosporium* pellets were seeded into 10 mL centrifuge tubes and 2,7-dichlorodihydrofluorescein-diacetate (H_2DCF-DA) (5 μM) was added for 2 h incubation. The medium was then removed and the pellets were treated with different concentrations of CdSe/ZnS QDs (0, 10, 20, 50, and 80 nM) for 24 h. After that, the pellets were washed with fresh phosphate-buffered saline (PBS) for three times and observed by confocal laser scanning microscopy (FV1,000, TY1,318, Japan) equipped with double photon detector.

2.6. Reactive oxygen species measurements

ROS was measured using H_2DCF-DA, as a fluorometric indicator previously described by Chen et al. [30]. H_2DCF-DA could be converted into 2,7-dichlorodihydrofluorescein (H_2DCF) by intracellular esterase, and intracellular ROS could transform H_2DCF into 2,7-dichlorofluorescein (DCF). Thus, the fluorescence intensity of

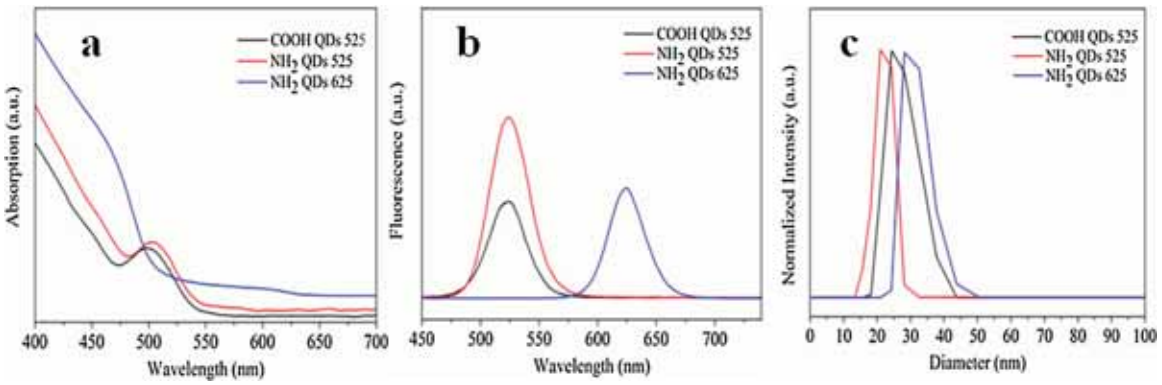

Fig. 1. Adsorption (a) and fluorescence (b) spectra of COOH QDs 525, NH_2 QDs 525, and NH_2 QDs 625 used in this work, and their representative DLS histograms (c). The concentrations of three CdSe/ZnS QDs were 20 nM.

DCF would indicate the degree of ROS generation. Before CdSe/ZnS QDs exposure, *P. chrysosporium* pellets were mixed with H_2DCF-DA (5 μM) and incubated for 2 h. The medium was then removed and the pellets were exposed to CdSe/ZnS QDs with different concentrations. The solution was then discarded, and the pellets were rinsed with PBS for fluorescence analysis using a fluorescence spectrometer (FluoroMax-4, Horiba Scientific, Japan) for excitation at 485 nm and emission at 525 nm.

2.7. Cell viability assays

Cell viability was measured using the colorimetric 3-(4,5-dimethylthiazol-2-yl)-2,5-diphenyltetrazolium bromide (MTT) assay according to the study reported by Luo et al. [12]. MTT is a yellow water-soluble tetrazolium dye, which can be transformed into a purple water-insoluble formazan by the living cells. And the content of purple formazan can directly reflect the proportion of living cells. Briefly, 0.2 g *P. chrysosporium* pellets were mixed with 1 mL MTT solution (5 g L^{-1}) and incubated at 50 °C for 2 h. The reaction was stopped by adding 0.5 mL hydrochloric acid (1 M) and the mixture was centrifuged at 10,000 rpm for 10 min using superspeed refrigerated centrifuge. The supernatant was discarded and the collected pellets were extracted in 6 mL propan-2-ol for 2 h. The centrifugation process was implemented again and the absorbance of the supernatant was recorded at 534 nm.

2.8. Statistical analysis

Statistical analysis was carried out in all assays. The tests were run three times and the results were presented as the mean of three replicates. A one-way analysis of variance (ANOVA) was performed with all samples, and p-values < 0.05 was deemed to be significantly different. All error bars represent one standard deviation (SD) of the arithmetic mean.

3. Results and discussion

3.1. The physicochemical characteristics of CdSe/ZnS QDs

To systematically investigate diameter and surface charges effects of CdSe/ZnS QDs on the bioaccumulation and toxicity to *P. chrysosporium*, three types of QDs with maximum luminescent wavelengths of 525 nm, 525 nm, and 625 nm were used in our experiment. The UV–vis absorption and fluorescence spectra of COOH CdSe/ZnS 525, NH_2 CdSe/ZnS 525, and NH_2 CdSe/ZnS 625 were shown in Fig. 1. It can be found that the first absorption maximums of COOH CdSe/ZnS 525, NH_2 CdSe/ZnS 525, and NH_2 CdSe/ZnS 625 were at 500 nm, 505 nm, and 600 nm, respectively (Fig. 1a). With an excitation wavelength of 380 nm, COOH CdSe/ZnS 525, NH_2 CdSe/ZnS 525, and NH_2 CdSe/ZnS 625 presented obvious and symmetrical fluorescence emission spectra with the emission maximums at 525 nm, 525 nm, and 625 nm without a tail (Fig. 1b), indicating that COOH CdSe/ZnS 525, NH_2 CdSe/ZnS 525, and NH_2 CdSe/ZnS 625 were nearly monodisperse and homogeneous. The zeta (ζ) potentials of COOH CdSe/ZnS 525, NH_2 CdSe/ZnS 525, and NH_2 CdSe/ZnS 625 were −15.8 mV, −6.4 mV, and −10.2 mV, respectively. As shown in Fig. 1c, hydrodynamic diameters of COOH CdSe/ZnS 525, NH_2 CdSe/ZnS 525, and NH_2 CdSe/ZnS 625 were 22.1 nm, 20.5 nm, and 27.4 nm, respectively, which were larger than those (5.6 nm, 5.2 nm, and 10.7 nm) determined by TEM (Fig. 2). The TEM images showed that the size distribution of QDs was uniform and the dispersancy was perfect. The deviation of diameter measured by DLS and TEM was ascribed to different surface states of nanoparticles under the tested conditions [36,37]. In details, QDs samples were directly tested in aqueous phase for DLS measurement while the solution must be strictly evaporated in TEM characterization.

3.2. Morphology analysis

The morphological analysis of hyphae in *P. chrysosporium* was implemented using SEM. As shown in Fig. 3, there are obvious morphological changes when in presence of 80 nM of COOH CdSe/ZnS 525, NH_2 CdSe/ZnS 525, and NH_2 CdSe/ZnS 625. The original hyphae of *P. chrysosporium* presented tight and intact shape (Fig. 3a) while it became incompact and granular after exposure to a high concentration (80 nM) of CdSe/ZnS QDs (Fig. 3b-d), indicating that the structure integrity of hyphae has been destroyed. Therefore, COOH CdSe/ZnS 525, NH_2 CdSe/ZnS 525, and NH_2 CdSe/ZnS 625 could induce toxicity in *P. chrysosporium* and cause structure damage of hyphae. In addition, the corresponding EDS images were shown in Fig. S1. It can be seen that the original hyphae of *P. chrysosporium* contained the elements of C, O, Na, P, Cl, and K. After incubation with CdSe/ZnS QDs, the elements of S, Zn, Se, and Cd in *P. chrysosporium* hyphae have been detected. Based on the results, it is obvious that CdSe/ZnS QDs have accumulated in the surface or inside of *P. chrysosporium* hyphae. And these adsorbed or accumulated CdSe/ZnS QDs have directly exerted an effect on the *P. chrysosporium* hyphae.

3.3. Confocal laser scanning microscopy analysis

In order to investigate the intracellular distribution of CdSe/ZnS QDs, the localization of COOH CdSe/ZnS 525, NH_2 CdSe/ZnS 525, and NH_2 CdSe/ZnS 625 in hyphae of *P. chrysosporium* were analyzed by confocal laser imaging. As shown in Fig. 4, the green fluorescence

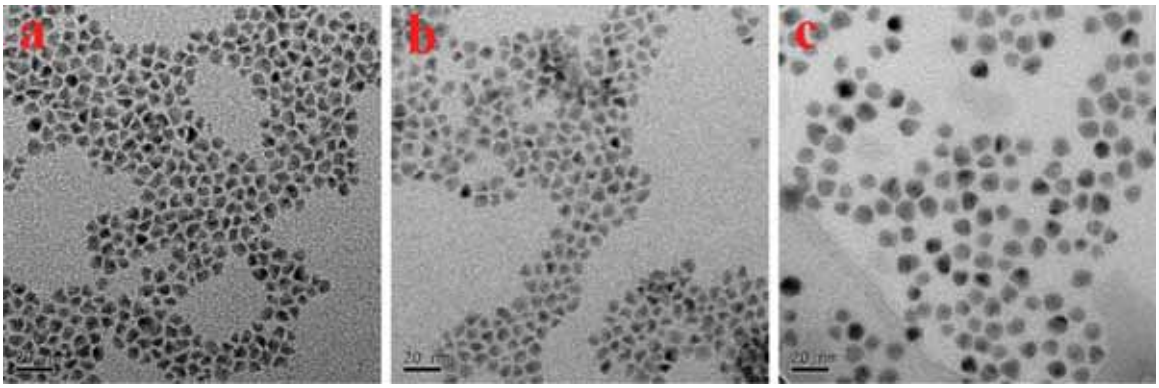

Fig. 2. TEM images of COOH CdSe/ZnS 525 (a), NH_2 CdSe/ZnS 525 (b), and NH_2 CdSe/ZnS 625 (c), respectively.

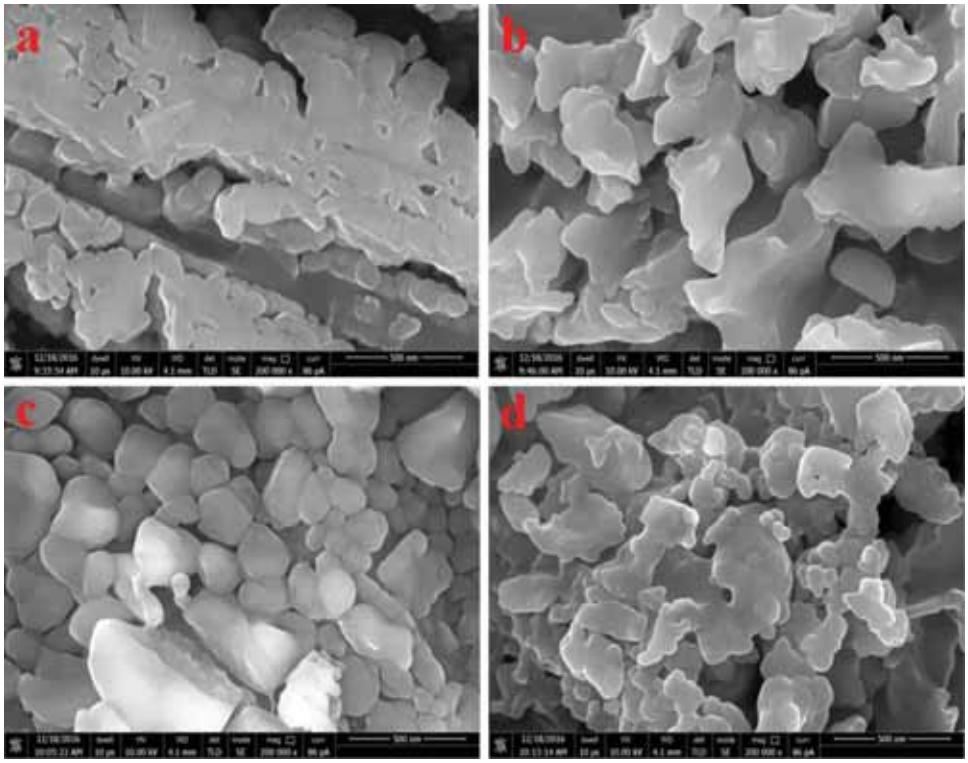

Fig. 3. Morphological analysis of hyphae in *P. chrysosporium* exposed to (a) control, (b) COOH CdSe/ZnS 525, (c) NH_2 CdSe/ZnS 525, and (d) NH_2 CdSe/ZnS 625 at concentration of 80 nM for 24 h by SEM (200, 000 × Objective), respectively.

channels represented the infected hyphae of *P. chrysosporium*, in which COOH CdSe/ZnS 525, NH_2 CdSe/ZnS 525, and NH_2 CdSe/ZnS 625 were largely accumulated. With an increase of concentrations from 10 nM to 80 nM, the accumulated amounts of CdSe/ZnS QDs also increased. To explore the potential roles of CdSe/ZnS QDs in inducing intracellular oxidative stress, the intracellular ROS generation was qualitatively analyzed by H_2DCF-DA assay coupled with confocal laser scanning microscopy. Fig. 4 showed that with an increase of CdSe/ZnS QDs concentrations from 10 nM to 80 nM, the fluorescent intensity in the hyphae of *P. chrysosporium* increased gradually, indicating that the intracellular ROS level also increased obviously. And all the evaluation results presented significant difference from control. Oxidative stress is one of the significant mechanisms of cytotoxicity induced by QDs [38,39]. The intracellular ROS would disturb the redox potential equilibrium, leading to an intracellular pro-oxidant environment, and ultimately cause the disruption of cell function [39]. In the present study, when CdSe/ZnS QDs entered to the hyphae of *P. chrysosporium* and accumulated largely in the hyphae, ROS was subsequently generated *in vivo*. Therefore, COOH CdSe/ZnS 525, NH_2 CdSe/ZnS 525, and NH_2 CdSe/ZnS 625 were proved to be toxic to *P. chrysosporium* in the tested concentration range.

3.4. Toxicity of CdSe/ZnS QDs to P. chrysosporium

QDs toxicity depends on multiple factors including its physicochemical properties and environmental conditions: size, surface charges, outer coating bioactivity (functional groups and capping material), inoculation concentration and time, and photolytic, oxidative, and mechanical stability. Previous studies demonstrated that the toxicity of CdSe/ZnS QDs to microorganisms could be attributed to the Cd^{2+} released from CdSe/ZnS QDs [25]. A recent report indicated that while CdSe/ZnS QDs and Cd^{2+} might have similar effects on microorganic survival, they had distinct mechanisms of toxicity [40].

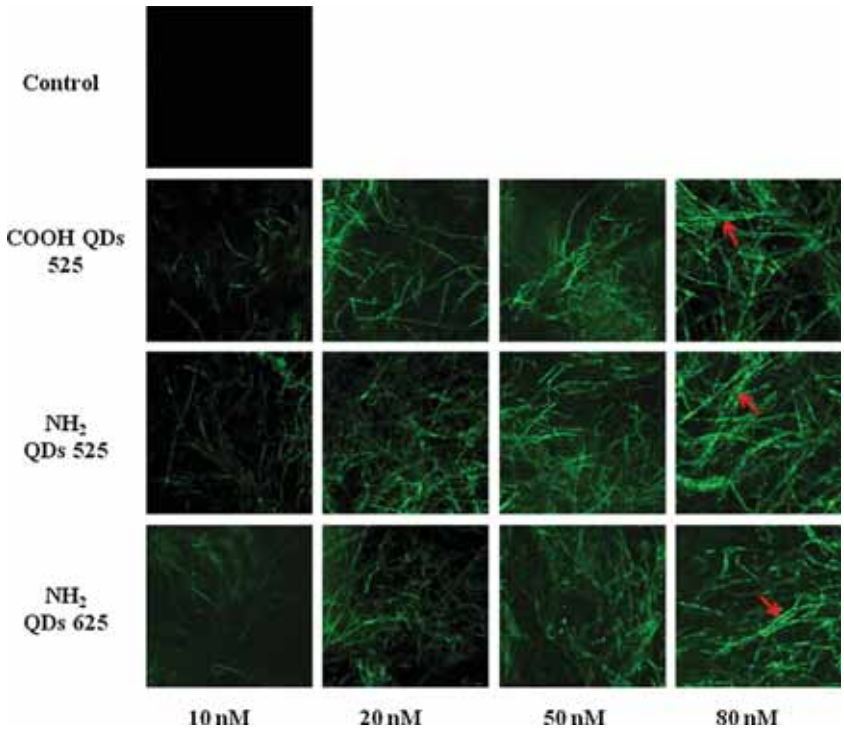

Fig. 4. Confocal laser scanning microscopy images of the hyphal localization (green fluorescence channel) of COOH CdSe/ZnS 525, NH_2 CdSe/ZnS 525, and NH_2 CdSe/ZnS 625, at concentrations of 10, 20, 50, and 80 nM, respectively. (For interpretation of the references to colour in this figure legend, the reader is referred to the web version of this article.)

3.4.1. Incubation concentrations

The toxicity of CdSe/ZnS QDs is the main reason that restricts their biomedical application. Thus, it is essential to systematically evaluate their biotoxicity, and herein the intracellular ROS level and the cell viability were investigated. In the present study, *P. chrysosporium* were incubated with different concentrations of COOH CdSe/ZnS 525, NH_2 CdSe/ZnS 525, and NH_2 CdSe/ZnS 625 (10 nM, 20 nM, 50 nM, and 80 nM for each QD) for 24 h, the intracellular ROS level and the cell viability of *P. chrysosporium* were measured, respectively. As shown in Fig. 5a-c, the intracellular ROS level of *P. chrysosporium* increased gradually with the increase concentrations of CdSe/ZnS QDs. However, the intracellular ROS levels of different CdSe/ZnS QDs treated *P. chrysosporium* were different under the identical conditions. For example, the intracellular ROS level of NH_2 CdSe/ZnS 525 treated *P. chrysosporium* overtopped 13% when the incubation concentration was 80 nM, which was greater than those of NH_2 CdSe/ZnS 625 (9%) and COOH CdSe/ZnS 525 (7.5%) treated *P. chrysosporium*. As shown in Fig. 5d-f, the cell viability of *P. chrysosporium* was decreased with the increase concentrations of CdSe/ZnS QDs. Similarly, the cell viabilities of different CdSe/ZnS QDs treated *P. chrysosporium* were distinctly different under the identical conditions. For instance, the cell viability of NH_2 CdSe/ZnS 525 treated *P. chrysosporium* decreased more than 36% when the incubation concentration was 80 nM, which was greater than those of NH_2 CdSe/ZnS 625 (21%) and COOH CdSe/ZnS 525 (15%) treated *P. chrysosporium*. For the two NH_2 CdSe/ZnS QDs, the results indicated the greater intracellular ROS level and lower cell viability were found in smaller NH_2 CdSe/ZnS 525 treated *P. chrysosporium* when compared with larger NH_2 CdSe/ZnS 625 treated samples. Because the smaller QDs were easier to be taken in by *P. chrysosporium* [41]. Due to the small particle size, CdSe/ZnS QDs could directly enter into the hyphae by several approaches such as macropinocytosis, caveolae-mediated endocytosis, and clathrin-mediated endocytosis [21]. Generally, the internalization process of CdSe/ZnS QDs includes the binding of CdSe/ZnS QDs to receptors on the plasma membrane surface and the generation of coated pits to deliver them to the intracellular area [42,43]. The amount of receptors on plasma membrane surface would determine the uptake of QDs. Meanwhile, the endocytosis is an energy-consuming process, smaller QDs would consume less energy than larger QDs, which may enhance the internalization effect [44]. In addition, due to the negative charges on cell membrane surface, the internalization amount of COOH CdSe/ZnS 525 was much less than that of NH_2 CdSe/ZnS 525. The larger negative charges made it more difficult for COOH CdSe/ZnS 525 to adsorb to cell membrane surface because of the electrostatic repulsion [41]. Therefore, the larger negative charged COOH CdSe/ZnS 525 caused lower toxicity to *P. chrysosporium*, and NH_2 CdSe/ZnS 525 with smaller size induced greater toxicity to *P. chrysosporium*.

The correlation analysis between intracellular ROS level and cell viability of *P. chrysosporium* and CdSe/ZnS QDs concentration was depicted in Fig. 6. As shown in Fig. 6a-c, the intracellular ROS levels of NH_2 CdSe/ZnS 525 and NH_2 CdSe/ZnS 625 treated *P. chrysosporium* increased gradually with an increase of CdSe/ZnS QDs concentrations in the culture medium, indicating that the intracellular ROS level was dose-dependent and the internalization amount of QDs increased with the increase of incubation concentrations. The intracellular ROS levels of NH_2 CdSe/ZnS 525 and NH_2 CdSe/ZnS 625 treated cells were partly correlated (R^2 = 0.97320 and R^2 = 0.86098, respectively) with the concentrations of CdSe/ZnS QDs (10 nM, 20 nM, 50 nM, and 80 nM). However, the intracellular ROS level of COOH CdSe/ZnS 525 treated cells was inferiorly correlated (R^2 = 0.50358) with the concentrations of CdSe/ZnS QDs, because the internalization amount of COOH CdSe/ZnS 525 was much lower than those of NH_2 CdSe/ZnS 525 and NH_2 CdSe/ZnS 625. Consequently, the lower internalization in *P. chrysosporium* may result in the lower intracellular ROS levels. Similarly, as shown in Fig. 6d-f, the cell viabilities of NH_2 CdSe/ZnS 525 and NH_2 CdSe/ZnS 625 treated *P. chrysosporium* decreased gradually with an increase of CdSe/ZnS QDs concentrations in the culture medium,

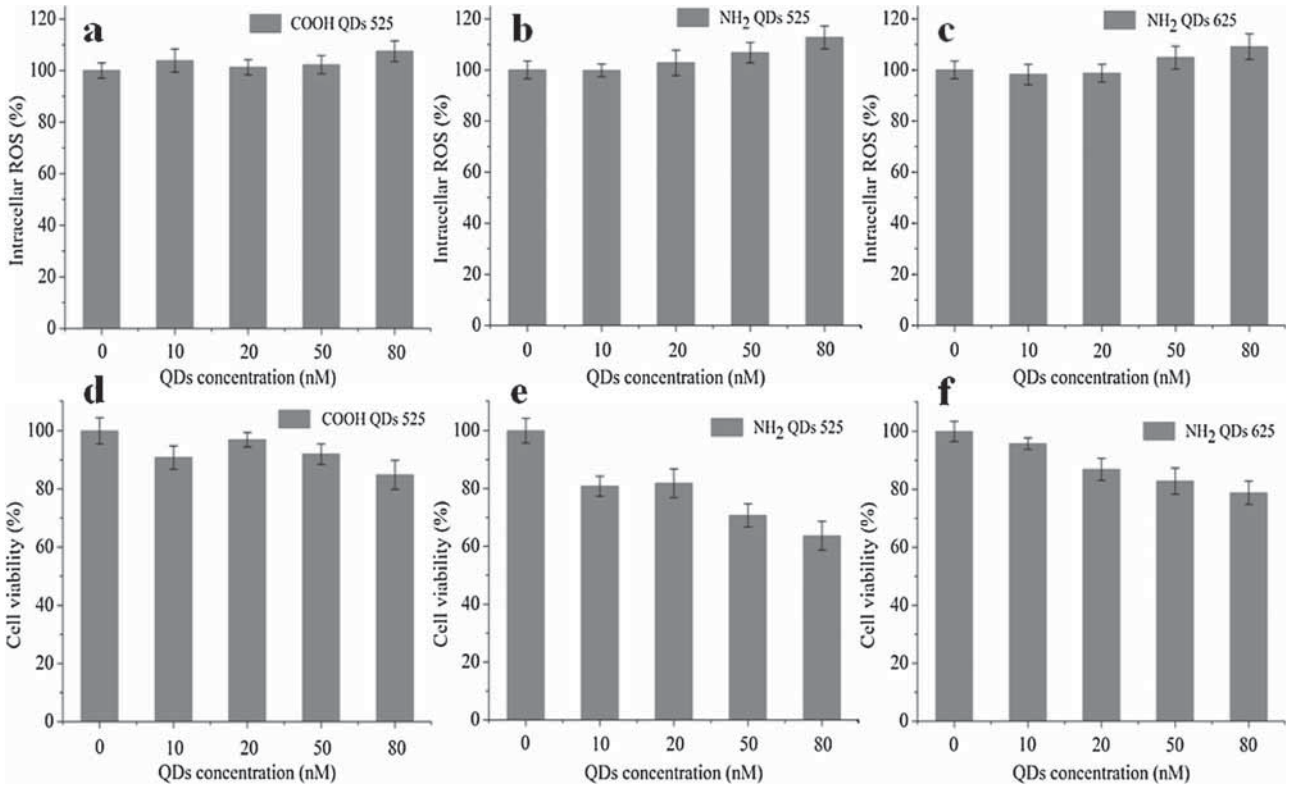

Fig. 5. Intracellular ROS level and cell viability of *P. chrysosporium* incubated with different concentrations of COOH CdSe/ZnS 525, NH_2 CdSe/ZnS 525, and NH_2 CdSe/ZnS 625 for 24 h. Error bars represent one SD of the arithmetic mean.

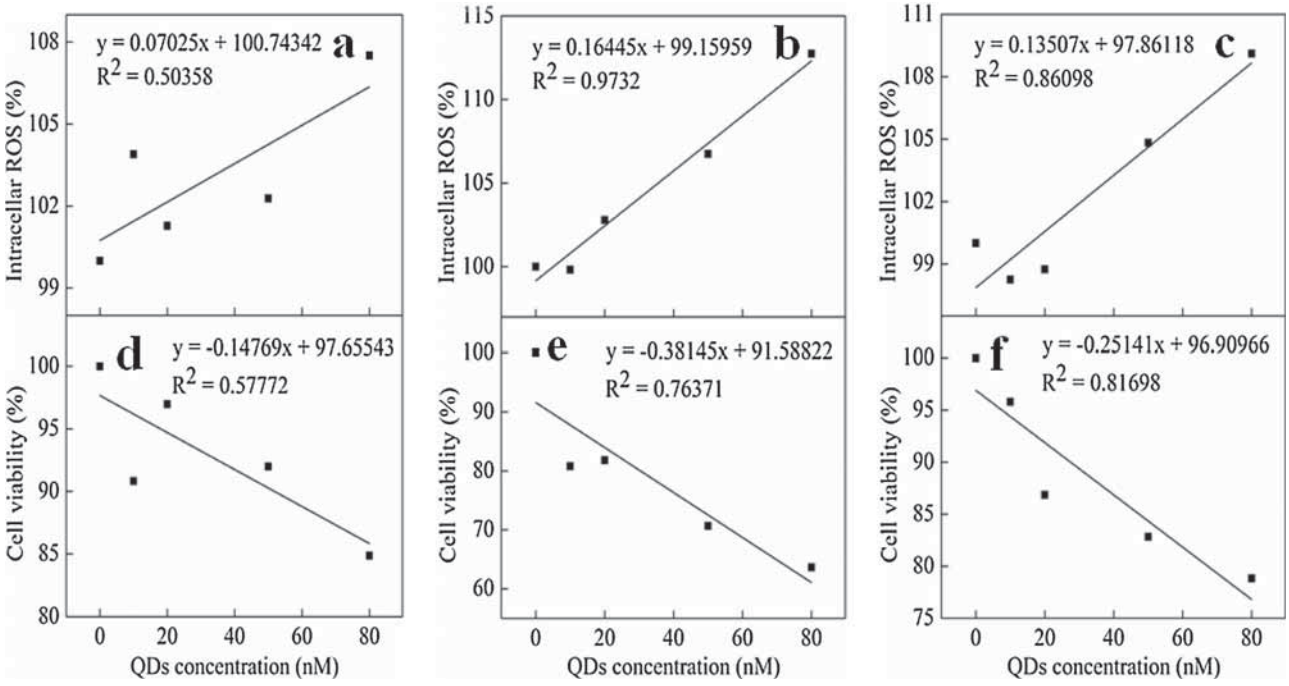

Fig. 6. Correlations between intracellular ROS level and cell viability of *P. chrysosporium* and QDs concentration in the medium. (a) and (d) represent COOH CdSe/ZnS 525, (b) and (e) represent NH_2 CdSe/ZnS 525, (c) and (f) represent NH_2 CdSe/ZnS 625, respectively.

demonstrating that the cell viability was also dose-dependent. The cell viabilities of NH_2 CdSe/ZnS 525 and NH_2 CdSe/ZnS 625 treated *P. chrysosporium* were partly correlated ($R^2 = 0.76371$ and $R^2 = 0.81698$, respectively) with the concentrations of CdSe/ZnS QDs (10 nM, 20 nM, 50 nM, and 80 nM). However, the cell viability of COOH CdSe/ZnS 525 treated *P. chrysosporium* was inferiorly correlated ($R^2 = 0.57772$) with the concentrations of CdSe/ZnS QDs, which demonstrated that the less internalization in *P. chrysosporium* may alleviate the decline of cell viability. Many cell toxicity researches have confirmed that QDs could undergo the exclusive

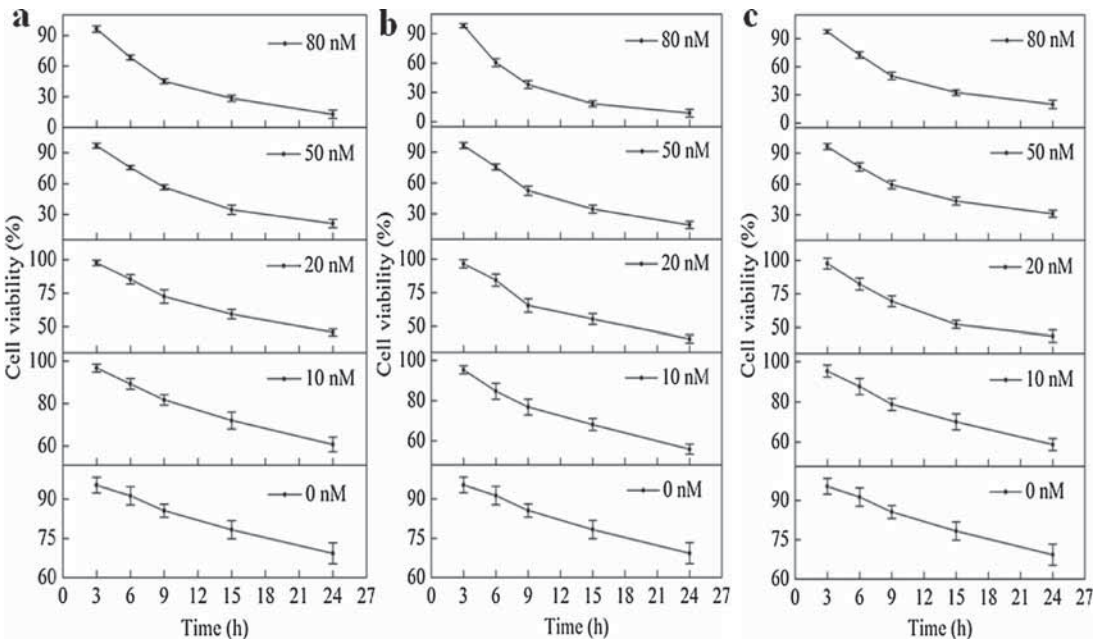

Fig. 7. Cell viability of *P. chrysosporium* exposed to (a) COOH CdSe/ZnS 525, (b) NH_2 CdSe/ZnS 525, and (c) NH_2 CdSe/ZnS 625 for different time and concentrations. Error bars represent one SD of the arithmetic mean.

intracellular localization and aggregate to the membranous structures and intracellular proteins, inducing the generation of ROS [45,46]. These QDs-induced ROS are recognized as a significant factor for causing the cytotoxicity. The generation mechanism of ROS is that photosensitive QDs could transfer electron to molecular oxygen in medium and cause the production of singlet oxygen, which may react with water or other molecules to excite the generation of ROS, including hydroxyl radical (·OH), superoxide anion (O_2^-), and hydrogen peroxide (H_2O_2) [47,48]. These free radicals were demonstrated to cause DNA nicking and break, metabolic functions loss, and apoptosis [13].

3.4.2. Incubation time

The incubation time plays a vital role in the bioaccumulation and toxicity of COOH CdSe/ZnS 525, NH_2 CdSe/ZnS 525, and NH_2 CdSe/ZnS 625 in *P. chrysosporium*. The cell viabilities of *P. chrysosporium* exposed to COOH CdSe/ZnS 525, NH_2 CdSe/ZnS 525, and NH_2 CdSe/ZnS 625 during 24 h were depicted in Fig. 7. The cell viabilities of *P. chrysosporium* were decreased with time in all CdSe/ZnS QDs treated samples. But the cell viabilities of different CdSe/ZnS QDs treated *P. chrysosporium* were obviously different under the identical conditions. For example, the cell viability of NH_2 CdSe/ZnS 525 treated *P. chrysosporium* decreased more than 89% at 24 h when the incubation concentration was 80 nM, which was greater than those of NH_2 CdSe/ZnS 625 (77%) and COOH CdSe/ZnS 525 (83%) treated *P. chrysosporium*. The cellular uptake of CdSe/ZnS QDs presented a time-dependent saturation since the internalization amount of CdSe/ZnS QDs finally reached a plateau. The membrane receptors for the uptake of CdSe/ZnS QDs were gradually consumed as time lapsed, and the internalization rate of CdSe/ZnS QDs would decline and eventually reach saturation [42,49]. In addition, the less negative charges and smaller size made it easier and faster for NH_2 CdSe/ZnS 525 to be adsorbed by *P. chrysosporium* [41,50]. With an increase concentration of CdSe/ZnS QDs, the decrease rate of cell viability increased in all CdSe/ZnS QDs treated samples. As the dose added, the concentration of CdSe/ZnS QDs on the membrane increased, and more CdSe/ZnS QDs could be taken up by *P. chrysosporium*, leading to the greater decrease rate of cell viability. Thus, the bioaccumulation and toxicity of CdSe/ZnS QDs in *P. chrysosporium* presented a dose-dependent and time-dependent process, which is in accordance with the previous studies reported by Misra et al. [51] and Nguyen et al. [52].

4. Conclusions

In summary, we comprehensively investigated the bioaccumulation and toxicity of three types of CdSe/ZnS QDs in *P. chrysosporium* by using confocal laser scanning microscopy, ROS measurements, and cell viability assays. Our results showed that the bioaccumulation and toxicity of CdSe/ZnS QDs in *P. chrysosporium* presented a dose-dependent and time-dependent process. After incubation by three types of CdSe/ZnS QDs with different particle sizes and functional groups (—COOH or —NH_2), we found that the cytotoxicity of QDs was related to their physicochemical properties: the small NH_2 CdSe/ZnS 525 was more cytotoxic than the large NH_2 CdSe/ZnS 625, and the smaller negative charged NH_2 CdSe/ZnS 525 resulted in greater cytotoxicity than the larger negative charged COOH CdSe/ZnS 525. Three CdSe/ZnS QDs were accumulated largely in the hyphae and exhibited toxicity to *P. chrysosporium* in the tested concentration range. Therefore, the potential risk of QDs to biosafety cannot be completely ruled out. Long-term studies must be implemented before QDs are routinely applied to the clinical medicine.

Acknowledgments

This work was financially supported by the National Natural Science Foundation of China (51521006, 51579099, 51508186, and 51378190), the Environmental Protection Technology Research Program of Hunan (2007185), the Program for Changjiang Scholars and Innovative Research Team in University (IRT-13R17) and Hunan Provincial Natural Science Foundation of China (2015JJ2031).

Appendix A. Supplementary data

Supplementary data associated with this article can be found, in the online version, at http://dx.doi.org/10.1016/j.colsurfb.2017.08.006.

References

[1] F. Ye, A. Barrefelt, H. Asem, M. Abedi-Valugerdi, I. El-Serafi, M. Saghafian, K. Abu-Salah, S. Alrokayan, M. Muhammed, M. Hassan, Biodegradable polymeric vesicles containing magnetic nanoparticles, quantum dots and anticancer drugs for drug delivery and imaging, Biomaterials 35 (2014) 3885–3894.

[2] T.Y. Rakovich, O.K. Mahfoud, B.M. Mohamed, A. Prina-Mello, K. Crosbie-Staunton, T. Van Den Broeck, L. De Kimpe, A. Sukhanova, D. Baty, A. Rakovich, Highly sensitive single domain antibody–quantum dot conjugates for detection of HER2 biomarker in lung and breast cancer cells, ACS Nano 8 (2014) 5682–5695.

[3] W.W. Tang, G.M. Zeng, J.L. Gong, Y. Liu, X.Y. Wang, Y.Y. Liu, Z.F. Liu, L. Chen, X.R. Zhang, D.Z. Tu, Simultaneous adsorption of atrazine and Cu (II) from wastewater by magnetic multi-walled carbon nanotube, Chem. Eng. J. 211 (2012) 470–478.

[4] W.W. Tang, G.M. Zeng, J.L. Gong, J. Liang, P. Xu, C. Zhang, B.B. Huang, Impact of humic/fulvic acid on the removal of heavy metals from aqueous solutions using nanomaterials: a review, Sci. Total Environ. 468 (2014) 1014–1027.

[5] H. Wang, X.Z. Yuan, Y. Wu, X.H. Chen, L.J. Leng, G.M. Zeng, Photodeposition of metal sulfides on titanium metal–organic frameworks for excellent visible-light-driven photocatalytic Cr (VI) reduction, RSC Adv. 5 (2015) 32531–32535.

[6] H. Wang, X.Z. Yuan, Y. Wu, G.M. Zeng, W.G. Tu, C. Sheng, Y.C. Deng, F. Chen, J.W. Chew, Plasmonic Bi nanoparticles and BiOCl sheets as cocatalyst deposited on perovskite-type $ZnSn(OH)_6$ microparticle with facet-oriented polyhedron for improved visible-light-driven photocatalysis, Appl. Catal. B: Environ. 209 (2017) 543–553.

[7] Z.Z. Wu, X.Z. Yuan, H. Wang, Z.B. Wu, L.B. Jiang, H. Wang, L. Zhang, Z.H. Xiao, X.H. Chen, G.M. Zeng, Facile synthesis of a novel full-spectrum-responsive $Co_{2.67}S_4$ nanoparticles for UV-, vis-and NIR-driven photocatalysis, Appl. Catal. B: Environ. 202 (2017) 104–111.

[8] P. Xu, G.M. Zeng, D.L. Huang, C.L. Feng, S. Hu, M.H. Zhao, C. Lai, Z. Wei, C. Huang, G.X. Xie, Use of iron oxide nanomaterials in wastewater treatment: a review, Sci. Total Environ. 424 (2012) 1–10.

[9] L. Tang, G.M. Zeng, G.L. Shen, Y.P. Li, Y. Zhang, D.L. Huang, Rapid detection of picloram in agricultural field samples using a disposable immunomembrane-based electrochemical sensor, Environ. Sci. Technol. 42 (2008) 1207–1212.

[10] M. Chu, X. Pan, D. Zhang, Q. Wu, J. Peng, W. Hai, The therapeutic efficacy of CdTe and CdSe quantum dots for photothermal cancer therapy, Biomaterials 33 (2012) 7071–7083.

[11] Y. Zhang, G.M. Zeng, L. Tang, D.L. Huang, X.Y. Jiang, Y.N. Chen, A hydroquinone biosensor using modified core–shell magnetic nanoparticles supported on carbon paste electrode, Biosens. Bioelectron. 22 (2007) 2121–2126.

[12] Y.H. Luo, S.B. Wu, Y.H. Wei, Y.C. Chen, M.H. Tsai, C.C. Ho, S.Y. Lin, C.S. Yang, P. Lin, Cadmium-based quantum dot induced autophagy formation for cell survival via oxidative stress, Chem. Res. Toxicol. 26 (2013) 662–673.

[13] A. Nagy, A. Steinbrück, J. Gao, N. Doggett, J.A. Hollingsworth, R. Iyer, Comprehensive analysis of the effects of CdSe quantum dot size, surface charge, and functionalization on primary human lung cells, Acs Nano 6 (2012) 4748–4762.

[14] J. Wan, G. Zeng, D. Huang, C. Huang, C. Lai, N. Li, Z. Wei, P. Xu, X. He, M. Lai, The oxidative stress of *Phanerochaete chrysosporium* against lead toxicity, Appl. Biochem. Biotech. 175 (2015) 1981–1991.

[15] P. Rivera-Gil, D. Jimenez De Aberasturi, V. Wulf, B. Pelaz, P. Del Pino, Y. Zhao, J.M. De La Fuente, I. Ruiz De Larramendi, T. Rojo, X.J. Liang, The challenge to relate the physicochemical properties of colloidal nanoparticles to their cytotoxicity, Accounts Chem. Res. 46 (2012) 743–749.

[16] L. Hu, G. Zeng, G. Chen, H. Dong, Y. Liu, J. Wan, A. Chen, Z. Guo, M. Yan, H. Wu, Treatment of landfill leachate using immobilized *Phanerochaete chrysosporium* loaded with nitrogen-doped TiO_2 nanoparticles, J. Hazard. Mater. 301 (2016) 106–118.

[17] X.J. Hu, J.S. Wang, Y.G. Liu, X. Li, G.M. Zeng, Z.L. Bao, X.X. Zeng, A.W. Chen, F. Long, Adsorption of chromium (VI) by ethylenediamine-modified cross-linked magnetic chitosan resin: isotherms, kinetics and thermodynamics, J. Hazard. Mater. 185 (2011) 306–314.

[18] S.J. Soenen, J. Demeester, S.C. De Smedt, K. Braeckmans, The cytotoxic effects of polymer-coated quantum dots and restrictions for live cell applications, Biomaterials 33 (2012) 4882–4888.

[19] Y. Su, Y. He, H. Lu, L. Sai, Q. Li, W. Li, L. Wang, P. Shen, Q. Huang, C. Fan, The cytotoxicity of cadmium based, aqueous phase-synthesized, quantum dots and its modulation by surface coating, Biomaterials 30 (2009) 19–25.

[20] M.D. Peterson, S.C. Jensen, D.J. Weinberg, E.A. Weiss, Mechanisms for adsorption of methyl viologen on CdS quantum dots, ACS Nano 8 (2014) 2826–2837.

[21] N.A. Al-Hajaj, A. Moquin, K.D. Neibert, G.M. Soliman, F.o.M. Winnik, D. Maysinger, Short ligands affect modes of QD uptake and elimination in human cells, ACS Nano 5 (2011) 4909–4918.

[22] T. Fan, Y. Liu, B. Feng, G. Zeng, C. Yang, M. Zhou, H. Zhou, Z. Tan, X. Wang, Biosorption of cadmium (II), zinc (II) and lead (II) by *Penicillium simplicissimum*: isotherms, kinetics and thermodynamics, J. Hazard. Mater. 160 (2008) 655–661.

[23] Y. Feng, J.L. Gong, G.M. Zeng, Q.Y. Niu, H.Y. Zhang, C.G. Niu, J.H. Deng, M. Yan, Adsorption of Cd (II) and Zn (II) from aqueous solutions using magnetic hydroxyapatite nanoparticles as adsorbents, Chem. Eng. J. 162 (2010) 487–494.

[24] G. Zeng, M. Chen, Z. Zeng, Risks of neonicotinoid pesticides, Science 340 (2013) 1403.

[25] R.F. Domingos, D.F. Simon, C. Hauser, K.J. Wilkinson, Bioaccumulation and effects of CdTe/CdS quantum dots on *Chlamydomonas reinhardtii*–nanoparticles or the free ions? Environ. Sci. Technol. 45 (2011) 7664–7669.

[26] D.L. Huang, G.M. Zeng, C.L. Feng, S. Hu, X.Y. Jiang, L. Tang, F.F. Su, Y. Zhang, W. Zeng, H.L. Liu, Degradation of lead-contaminated lignocellulosic waste by *Phanerochaete chrysosporium* and the reduction of lead toxicity, Environ. Sci. Technol. 42 (2008) 4946–4951.

[27] J. Wan, C. Zhang, G. Zeng, D. Huang, L. Hu, C. Huang, H. Wu, L. Wang, Synthesis and evaluation of a new class of stabilized nano-chlorapatite for Pb immobilization in sediment, J. Hazard. Mater. 320 (2016) 278–288.

[28] G. Zeng, M. Chen, Z. Zeng, Shale gas: surface water also at risk, Nature 499 (2013) 154.

[29] J.L. Gong, B. Wang, G.M. Zeng, C.P. Yang, C.G. Niu, Q.Y. Niu, W.J. Zhou, Y. Liang, Removal of cationic dyes from aqueous solution using magnetic multi-wall carbon nanotube nanocomposite as adsorbent, J. Hazard. Mater. 164 (2009) 1517–1522.

[30] A. Chen, G. Zeng, G. Chen, L. Liu, C. Shang, X. Hu, L. Lu, M. Chen, Y. Zhou, Q. Zhang, Plasma membrane behavior, oxidative damage, and defense mechanism in *Phanerochaete chrysosporium* under cadmium stress, Process Biochem. 49 (2014) 589–598.

[31] G. Chen, B. Yi, G. Zeng, Q. Niu, M. Yan, A. Chen, J. Du, J. Huang, Q. Zhang, Facile green extracellular biosynthesis of CdS quantum dots by white rot fungus *Phanerochaete chrysosporium*, Colloids Surf. B: Biointerfaces 117 (2014) 199–205.

[32] L. Hu, Y.T. Liu, G.M. Zeng, G.Q. Chen, J. Wan, Y.X. Zeng, L.L. Wang, H.P. Wu, P. Xu, C. Zhang, M. Cheng, T.J. Hu, Organic matters removal from landfill leachate by immobilized *Phanerochaete chrysosporium* loaded with graphitic carbon nitride under visible light irradiation, Chemosphere 184 (2017) 1071–1079.

[33] G.M. Zeng, J. Wan, D.L. Huang, L. Hu, C. Huang, M. Cheng, W.J. Xue, X.M. Gong, R.Z. Wang, D.N. Jiang, Precipitation, adsorption and rhizosphere effect: the mechanisms for Phosphate-induced Pb immobilization in soils – a review, J. Hazard. Mater. 339 (2017) 354–367.

[34] Y. He, H.T. Lu, L.M. Sai, Y.Y. Su, M. Hu, C.H. Fan, W. Huang, L.H. Wang, Microwave synthesis of water-dispersed CdTe/CdS/ZnS core-shell–shell quantum dots with excellent photostability and biocompatibility, Adv. Mater. 20 (2008) 3416–3421.

[35] T.K. Kirk, E. Schultz, W. Connors, L. Lorenz, J. Zeikus, Influence of culture parameters on lignin metabolism by *Phanerochaete chrysosporium*, Arch. Microbiol. 117 (1978) 277–285.

[36] Y. Su, F. Peng, Z. Jiang, Y. Zhong, Y. Lu, X. Jiang, Q. Huang, C. Fan, S.T. Lee, Y. He, In vivo distribution, pharmacokinetics, and toxicity of aqueous synthesized cadmium-containing quantum dots, Biomaterials 32 (2011) 5855–5862.

[37] Z. Huang, G. Chen, G. Zeng, Z. Guo, K. He, L. Hu, J. Wu, L. Zhang, Y. Zhu, Z. Song, Toxicity mechanisms and synergies of silver nanoparticles in 2, 4-dichlorophenol degradation by *Phanerochaete chrysosporium*, J. Hazard. Mater. 321 (2017) 37–46.

[38] E.Q. Contreras, M. Cho, H. Zhu, H.L. Puppala, G. Escalera, W. Zhong, V.L. Colvin, Toxicity of quantum dots and cadmium salt to *Caenorhabditis elegans* after multigenerational exposure, Environ. Sci. Technol. 47 (2012) 1148–1154.

[39] L. Peng, M. He, B. Chen, Y. Qiao, B. Hu, Metallomics study of CdSe/ZnS quantum dots in HepG2Cells, ACS Nano 9 (2015) 10324–10334.

[40] P.N. Wiecinski, K.M. Metz, T.C. King Heiden, K.M. Louis, A.N. Mangham, R.J. Hamers, W. Heideman, R.E. Peterson, J.A. Pedersen, Toxicity of oxidatively degraded quantum dots to developing zebrafish (*Danio rerio*), Environ. Sci. Technol. 47 (2013) 9132–9139.

[41] S.J. Tan, N.R. Jana, S. Gao, P.K. Patra, J.Y. Ying, Surface-ligand-dependent cellular interaction subcellular localization, and cytotoxicity of polymer-coated quantum dots, Chem. Mater. 22 (2010) 2239–2247.

[42] S. Ohta, S. Inasawa, Y. Yamaguchi, Real time observation and kinetic modeling of the cellular uptake and removal of silicon quantum dots, Biomaterials 33 (2012) 4639–4645.

[43] H. Wu, C. Lai, G. Zeng, J. Liang, J. Chen, J. Xu, J. Dai, X. Li, J. Liu, M. Chen, The interactions of composting and biochar and their implications for soil amendment and pollution remediation: a review, Crit. Rev. Biotechnol. (2016) 1–11.

[44] X. Jiang, C. Röcker, M. Hafner, S. Brandholt, R.M. Dörlich, G.U. Nienhaus, Endo-and exocytosis of zwitterionic quantum dot nanoparticles by live HeLa cells, ACS Nano 4 (2010) 6787–6797.

[45] L. Hu, C. Zhang, G. Zeng, G. Chen, J. Wan, Z. Guo, H. Wu, Z. Yu, Y. Zhou, J. Liu, Metal-based quantum dots: synthesis, surface modification, transport and fate in aquatic environments and toxicity to microorganisms, RSC Adv. 6 (2016) 78595–78610.

[46] S.J. Soenen, B.B. Manshian, T. Aubert, U. Himmelreich, J. Demeester, S.C. De Smedt, Z. Hens, K. Braeckmans, Cytotoxicity of cadmium-free quantum dots and their use in cell bioimaging, Chem. Res. Toxicol. 27 (2014) 1050–1059.
[47] A. Nagy, A. Zane, S.L. Cole, M. Severance, P.K. Dutta, W.J. Waldman, Contrast of the biological activity of negatively and positively charged microwave synthesized CdSe/ZnS quantum dots, Chem. Res. Toxicol. 24 (2011) 2176–2188.
[48] A. Nagy, J.A. Hollingsworth, B. Hu, A. Steinbrück, P.C. Stark, C. Rios Valdez, M. Vuyisich, M.H. Stewart, D.H. Atha, B.C. Nelson, Functionalization-dependent induction of cellular survival pathways by CdSe quantum dots in primary normal human bronchial epithelial cells, ACS Nano 7 (2013) 8397–8411.
[49] L. Peng, M. He, B. Chen, Q. Wu, Z. Zhang, D. Pang, Y. Zhu, B. Hu, Cellular uptake, elimination and toxicity of CdSe/ZnS quantum dots in HepG2 cells, Biomaterials 34 (2013) 9545–9558.
[50] D. Mo, L. Hu, G. Zeng, G. Chen, J. Wan, Z. Yu, Z. Huang, K. He, C. Zhang, M. Cheng, Cadmium-containing quantum dots: properties, applications, and toxicity, Appl. Microbiol. Biotechnol. 101 (2017) 2713–2733.
[51] S. Misra, R.W. Kwong, S. Niyogi, Transport of selenium across the plasma membrane of primary hepatocytes and enterocytes of rainbow trout, J. Exp. Biol. 215 (2012) 1491–1501.
[52] K.C. Nguyen, W.G. Willmore, A.F. Tayabali, Cadmium telluride quantum dots cause oxidative stress leading to extrinsic and intrinsic apoptosis in hepatocellular carcinoma HepG2 cells, Toxicology 306 (2013) 114–123.